Decay instability at the ion-sound frequency induced by a large amplitude Bernstein mode in a plasma

1971 J. Phys. A: Gen. Phys. 4 L67

(http://iopscience.iop.org/0022-3689/4/4/002)

We have also considered the case of oblique wave propagation, $\boldsymbol{k}.\boldsymbol{B} \neq 0$, where, as Gary (1970) has shown, the instability is ion acoustic. We find a similar result to equation (8)

$$R = 1 + \frac{3v_T}{2(v_d - \omega_R/k_y)}$$

but ω_R is here given by the ion acoustic frequency (Sanderson and Priest 1971). These results confirm the prediction of Woods (1969) that in strong shocks the large temperature gradient should play a dominant role. A fuller account of this work including a discussion of the ∇B terms will be given in a subsequent paper.

We should like to thank Professor L. C. Woods and Drs R. A. Cairns, S. P. Gary, M. Keilhacker, C. N. Lashmore-Davies and J. W. M. Paul for helpful comments and discussions.

Department of Applied Mathematics
University of St. Andrews
St. Andrews
Fife, Scotland

J J Sanderson
E R Priest
13*th April* 1971

Gary, S. P., 1970, *J. Plasma Phys.*, **4**, 753–60.
Gary, S. P., and Biskamp, D., 1971, *J. Phys.* A: *Gen. Phys.*, **4**, L27–30.
Gary, S. P., and Sanderson, J. J., 1970, *J. Plasma Phys.*, **4**, 739–51.
Keilhacker, M., Kornherr, M., and Steuer, K. H., 1969, *Z. Phys.*, **223**, 385–96.
Krall, N. A., 1968, *Advances in Plasma Physics*, Vol. 1 (New York: Interscience), p. 158.
Lashmore-Davies, C. N., 1970, *J. Phys.* A: *Gen. Phys.*, **3**, L40–5.
Sanderson, J. J., and Priest, E. R., 1971, (submitted to 10*th Int. Conf. on Phenomena in Ionized Gases, Oxford*).
Wong, H. V., 1970, *Phys. Fluids*, **13**, 757–60.
Woods, L. C., 1969, *Phys. Fluids*, **12**, 1635–41.

Decay instability at the ion-sound frequency induced by a large amplitude Bernstein mode in a plasma

Abstract. Experimental results are presented which show that a large-amplitude wave of one of the Bernstein modes, above a certain threshold power, can decay into another Bernstein mode plus a low frequency ion-sound wave. At larger incident amplitudes, a whole spectrum of low-frequency ion waves was observed, with frequencies extending up to the ion plasma frequency. These results are compared with a previous theory and reasonable agreement is achieved.

Recently, the parametric excitation of various plasma waves has been of considerable interest both theoretically (Dubois and Goldman 1965, Silin 1965, Jackson 1967, Tzoar 1969, Pomeau 1967) and experimentally (Stern and Tzoar 1966, Hiroe and Ikegami 1967, Stern 1969, Porkolab and Chang 1969, Wong *et al.* 1970). In particular, the nonlinear coupling of high-frequency electric fields to low-frequency density oscillations in a plasma has been demonstrated in a number of cases (Stern and Tzoar 1966, Hiroe and Ikegami 1967, Stern 1969, Wong *et al.* 1970). This experiment reports the situation in which the high-frequency electric field induces a Bernstein mode (Bernstein 1958) at frequency ω_0 close to the electron–cyclotron resonance (ecr) frequency ω_c, and the nonlinear coupling transfers energy to another Bernstein mode at a lower frequency ω_1, plus a low-frequency mode ω_2, which in this case is the ion-sound decay instability ω_s. This decay process requires the following relationships between the frequencies $\omega(k)$, and wavenumber $\bar{k}$, to be satisfied:

$$\omega_0(k_0) = \omega_1(k_1) + \omega_2(k_2) \tag{1}$$

$$\boldsymbol{k}_0 = \boldsymbol{k}_1 + \boldsymbol{k}_2 \tag{2}$$

where ω_0 is the incident Bernstein mode, $\omega_1 = (\omega_0 - \omega_s)$ is another Bernstein mode, and $\omega_2 = \omega_s$ is the resultant decay instability at the ion-sound frequency. The relationship between the wavenumbers demands that $\bar{k}_1 = \bar{k}_0 - \bar{k}_s$. Equations (1) and (2) are given simply by the conservation of energy and momentum relationships, respectively.

The experiments were performed in an E-type (capacitively coupled) rf discharge ($f \sim 27$ MHz) which, by varying the input power, gave peak densities in the range 10^9–10^{10} cm^{-3}. This discharge was run in a homogeneous ($\sim \frac{1}{2}\%$) axial magnetic field which was varied between 0·1 and 1·0 kG, (thus varying the ecr frequency between approximately 0·28 and 2·8 GHz) and was contained in a glass tube. The electron temperature T_e was much greater than the ion temperature T_i, and varied between 3·5 and 12·5 eV depending upon the rf discharge power input, or the neutral gas used (either hydrogen, helium, neon or argon). This electron temperature was measured using a double-probe technique. The electron density n was obtained from the double-probe measurements or, alternatively, from the frequency shift in the resonant frequency of a TM_{010} mode coaxial microwave cavity (Buchsbaum and Brown 1957). A further check of density was afforded by a measurement of the upper hybrid frequency $\omega_{UH} = (\omega_c{}^2 + \omega_p{}^2)^{1/2}$, where ω_p is the electron plasma frequency. All three methods were in good agreement.

Externally applied signals were coupled to the plasma using a Lisitano (1966) slot line cavity device outside the glass discharge tube or by a probe inserted into the plasma. The high-frequency signals were detected either by a radially movable probe inserted into the plasma or by a loop aerial outside the discharge tube. The low-frequency 'instabilities' were detected on a radially movable probe which could be used in its floating or ion-based configuration, or by the modulation effect produced by these density oscillations on incident microwave radiation (at 1·060 GHz) from the same cavity as used for the density measurements (Wong *et al.* 1970).

In these experiments, a uhf signal of frequency ω_0 was fed to the Lisitano 'coil' and, if the magnetic field was varied such that ω_0/ω_c was in the range 1·05–1·25, Bernstein modes propagated in the plasma. At low power inputs a spectral analysis near ω_0 (figure 1(*a*)) showed a single frequency at ω_0 in the radiation emitted by the plasma. Figure 1(*d*) shows the corresponding low-frequency spectrum between 0 and 1 MHz taken at the same power input. When the incident power at ω_0 was increased above a certain threshold value, the plasma was found to emit radiation at two additional frequencies: $\omega_0 - \omega_s$ and $\omega_0 + \omega_s$, as can be seen in figure 1(*b*). In this experiment the signal at $\omega_0 - \omega_s$ was always at least one order of magnitude higher in amplitude than the signal at $\omega_0 + \omega_s$. The corresponding low-frequency spectrum is

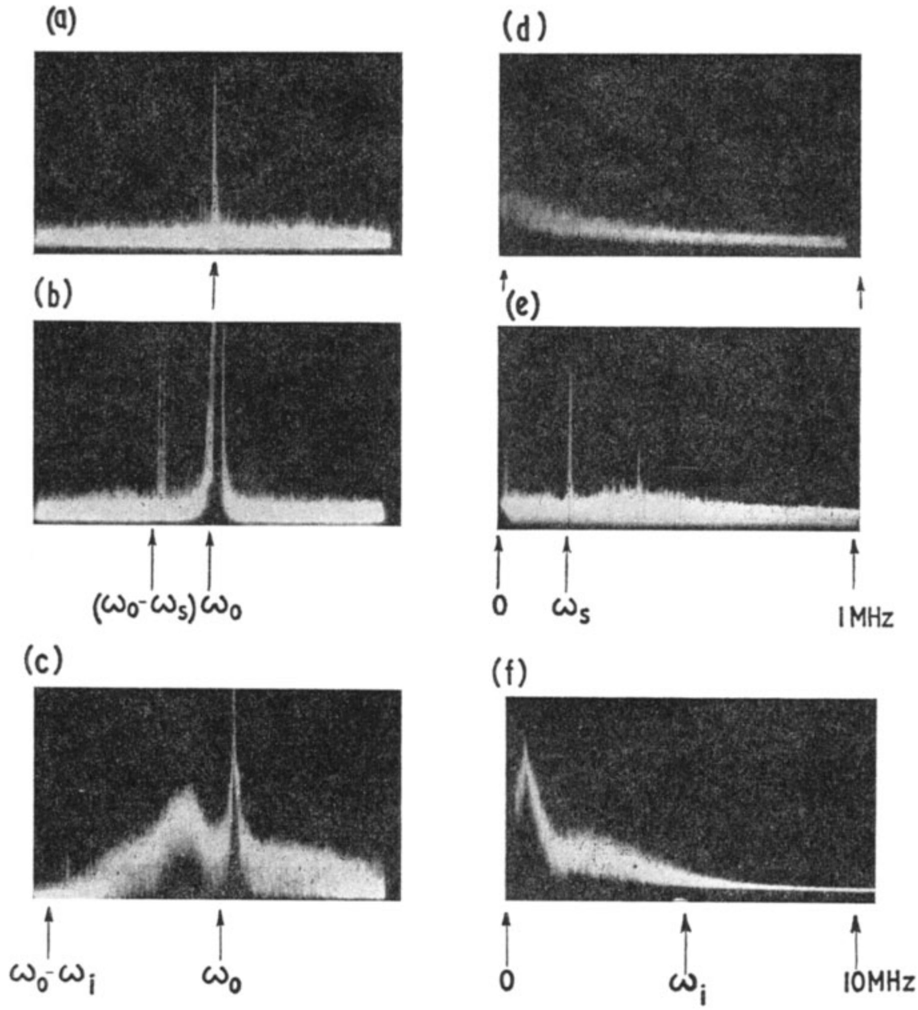

Figure 1. Spectral analysis of parametrically excited plasma oscillations in a helium plasma for $\omega_c \simeq 500$ MHz, $\omega_0/\omega_c \simeq 1{\cdot}14$ and $\omega_p/\omega_c \simeq 1{\cdot}0$. (*a*) high-frequency (hf) spectrum near ω_0; (*d*) low-frequency (lf) spectrum. Both (*a*) and (*d*) are for power inputs below threshold value. (*b*) hf spectrum near ω_0; (*e*) lf spectrum. Both (*b*) and (*e*) are for power inputs above threshold value. (*a*), (*b*), (*d*) and (*e*) have dispersion 100 kHz/div, and linear vertical scales. (*c*) hf spectrum near ω_0; (*f*) lf spectrum. Both (*c*) and (*e*) have dispersion 1 MHz/div, log scales vertically, and are for input powers much above threshold.

shown in figure 1(*e*), and this shows also a spectral component appearing at ω_s. These particular experiments were carried out in a helium plasma, with $\omega_0 = 500$ MHz; the low-frequency component appeared at $\omega_s \simeq 200$ kHz, $\omega_0/\omega_c \simeq 1{\cdot}14$, and $\omega_p/\omega_c \simeq 1$ for that plasma density at the centre of the tube.

The possible low-frequency ion-waves are given by the following dispersion relationship for an infinite plasma (Crawford 1961):

$$\omega^2 = \omega_i^2/\{1+(\omega_i^2 M_i/k^2 T_e)\} \tag{3}$$

where $\omega_i = (4\pi n e^2/M_i)^{1/2}$ is the ion plasma frequency, and M_i is the ion mass. For radial waves, it has been shown (Crawford 1961) that, in a bounded plasma, there is a low-frequency cut-off given by

$$\omega_s = (2{\cdot}405/\pi d)(T_e/M_i)^{1/2} \tag{4}$$

where d is the diameter of the containing tube. There is, also, an upper frequency cut-off in the short-wavelength ($= 2\pi/k$) limit given by

$$\omega = \omega_i. \tag{5}$$

In order to see if the measured low-frequency corresponded to the value given by equation (4), the experiment was repeated in four different plasmas (hydrogen, helium, neon and argon), thus varying both T_e and M_i. A further check was afforded by repeating the experiment in three different diameter tubes, namely $d = 6{\cdot}2$, $5{\cdot}0$ and $2{\cdot}5$ cm respectively. Figure 2(a) shows the result of these experiments plotted as the measured low-frequency ω_m against the calculated value $\omega_s = (2{\cdot}405/\pi d)(T_e/M_i)^{1/2}$.

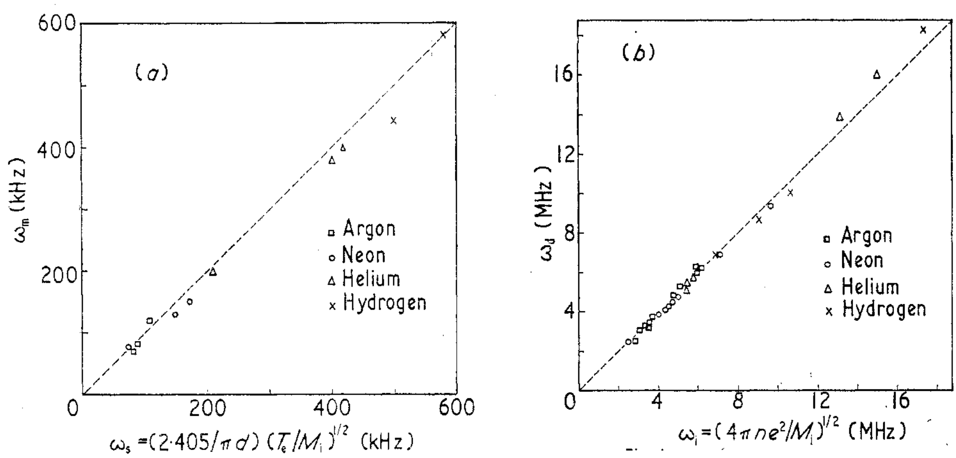

Figure 2. (a) The measured decay instability frequency ω_m plotted against the theoretical value $\omega_s = (2{\cdot}405/\pi d)(T_e/M_i)^{1/2}$ (b) the measured cut-off frequency ω_d plotted against the theoretical value $\omega_i = (4\pi n e^2/M_i)^{1/2}$, for input powers much above threshold.

Good agreement is obtained, and thus it is inferred that it is the radial ion sound wave instability which is excited.

These experiments were performed at various input frequencies between 0·28 and 2·8 GHz, and the magnetic field was varied such that the Bernstein mode was propagated. In each case a threshold incident power value was required before excitation at ω_s appeared. Corresponding to the spectra in figure 1, a plot of the ion-sound wave amplitude against the incident power at ω_0($= 500$ MHz) is shown in figure 3(a). It is clearly seen that a threshold value of about 5 watts ($E \sim 30$ V cm^{-1}) is required for excitation of ω_s(~ 200 kHz). As the power level is further increased the instability amplitude increases but begins to saturate at higher power levels (~ 10 watts). At these levels it was noticed that other modes were excited and a more 'turbulent' spectrum was apparent. Figure 1(c) shows a spectral analysis near ω_0 (with a logarithmic vertical scale of approximately 10 dB/div) and in this case

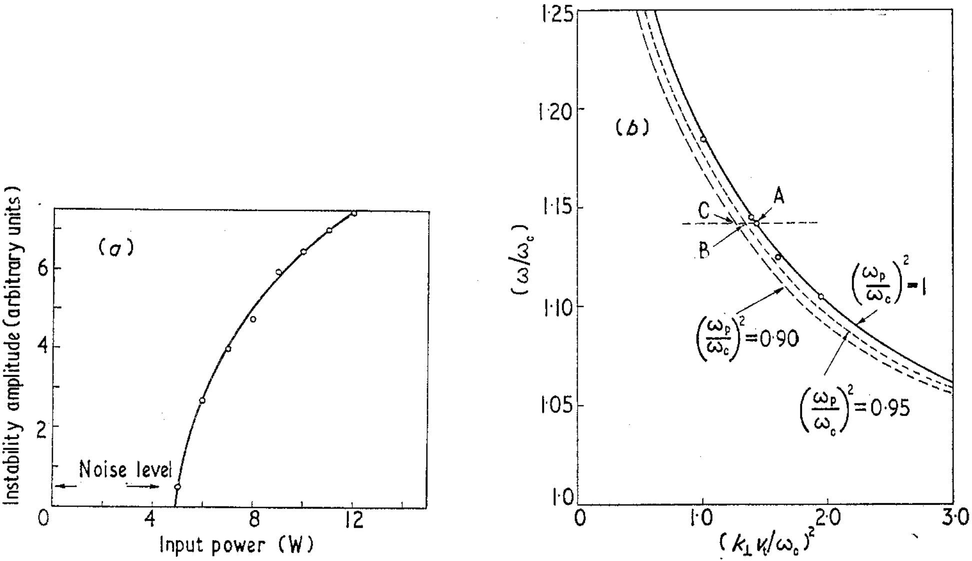

Figure 3. (*a*) Instability amplitude plotted against power input to the Lisitano structure, and (*b*) (ω/ω_c) plotted against $(k_\perp v_t/\omega_c)^2$. The open circles are experimental points and the full line is the theoretical curve.

there appears to be a lower sideband with a whole range of frequencies from $\omega_0 - \omega_s$ down to a cut-off frequency at $\omega_0 - \omega_i$. The corresponding low-frequency spectrum (0–10 MHz) is shown, with a logarithmic vertical scale, in figure 1(*f*). Experiments were carried out in various plasmas, varying the central plasma density in each case, to measure this cut-off frequency $(\omega_0 - \omega_d)$. This is shown plotted in figure 2(*b*) as the measured cut-off (ω_d) against the theoretical value $\omega_i = (4\pi n\, e^2/M_i)^{1/2}$. Again, good agreement is apparent and in these conditions ion-sound waves in the range from the lower cut-off ω_s to the upper cut-off frequency ω_i are obtained.

Tzoar (1969) has considered the problem of parametric excitation of ion-sound waves from the decay of Bernstein modes, in which the electronic and ionic motions are coupled by the induced electric fields in the plasma. He has shown that this decay process is possible when equations (1) and (2) are satisfied and that in this case the growth rate γ for the low-frequency mode is given by

$$\gamma \simeq \tfrac{1}{4}\left(1 - \frac{\epsilon_\infty}{\epsilon_0}\right)\left(\frac{ek_0E_0}{m{\omega_p}^2}\right)\left(\frac{\omega_S{\omega_p}^2}{\omega_0}\right)^{1/2} - (\gamma_B\gamma_S)^{1/2} \qquad (6)$$

where E_0 is the transverse electric field of the Bernstein mode, m is the electron mass, γ_B and γ_S are the effective dissipation rates of the Bernstein and the ion-sound modes respectively, and ϵ_∞ and ϵ_0 are the dielectric constants of the Bernstein mode at infinite and zero frequencies respectively (Bernstein 1958).

It is apparent from photographs such as those in figure 1 that the conservation of energy (equation (1)) is satisfied in the process. A check of conservation of momentum (equation (2)) proved to be a more difficult experiment. The Bernstein mode dispersion diagram was checked near to the conditions under which the photographs in figure 1 were obtained by using an interferometric technique. The resulting experimental points are shown plotted in figure 3(*b*) on the ω/ω_c against $(k_\perp v_t/\omega_c)^2$ curve (here $k_\perp$ was the radial wavenumber and $v_t = (T_e/m)^{1/2}$ was the electron thermal velocity). The full curve shows the theoretical curve (Bernstein 1965) for the case $(\omega_p/\omega_c)^2 \simeq 1$, which corresponds to the central plasma density in this case. The point A on the curve corresponds to the value $\omega_0 = 500$ MHz (i.e. figure 1). The resulting instability at ω_s was checked using the radial moving probe, and its wavenumber $k_2 = k_s$ was found. For the wave at $\omega_1 = \omega_0 - \omega_s$, the proximity of the large-amplitude wave at ω_0 swamped this wave at $(\omega_0 - \omega_s)$ and, consequently, a direct measure of its wavenumber k_1 was not possible. If it is assumed that this wave is also a Bernstein mode, it is not possible to satisfy equation (2) for both the high-frequency waves on the same branch of the full curve (figure 3(*b*)) since the slope of this curve $\Delta\omega/\Delta k$ is much less than $(\omega_0 - \omega_1)/(k_0 - k_1) = \omega_s/k_s$. However, a plausible explanation which will satisfy equation (2) is the following. Since the density n is a function of the plasma radius r, $n = n(r)$, it follows that the Bernstein mode dispersion curve is also a function of radius. Figure 3(*b*) shows the theoretical broken curves calculated for $(\omega_p/\omega_c)^2 = 0{\cdot}95$ and $0{\cdot}90$. Therefore, if the large-amplitude Bernstein wave at ω_0, k_0 (point A) decays to another one at $\omega_1 = (\omega_0 - \omega_s)$, $k_1 = (k_0 - k_s)$ (point B) (corresponding to the dispersion relationship at a slightly larger radius), then both equations (1) and (2) can be satisfied simultaneously, in an inhomogeneous plasma. Further decay from B to C, etc., will also satisfy these equations. A decay mode from C to B or B to A, etc., creates a Bernstein mode at $\omega_0 + \omega_s$, $k_0 + k_s$, but with a smaller probability than the lower sideband (Tsytovich 1970). In the same way, equations (1) and (2) may be satisfied simultaneously, at any (ω, k) related by the dispersion relationship equation (3), within the range ω_s to ω_i, by using a similar argument.

The possibility was considered that the input power creating the large-amplitude Bernstein wave created a non-Maxwellian distribution in the plasma, which in turn caused the low-frequency instability. This possibility was reduced by exciting a low-frequency wave (frequency $\omega' \simeq 50$ kHz) in the plasma and observing the 'mixing effects' produced with the Bernstein mode, below threshold. In this case, the upper and lower sidebands at $\omega_0 + \omega'$ and $\omega_0 - \omega'$ were observed of *equal* amplitude and an order of magnitude lower in amplitude than in previous experiments. This is contrary to that expected from decay instability theory (Tsytovich 1970) and the experimental observations. Also from equation (6), the threshold value for E_0 may be obtained by equating γ to zero and substituting for $\gamma_s = \nu_i$ as the ion–neutral collision frequency, and for γ_B as the measured decay value in the plasma. In this way a value of $E_0 \simeq 50$ V cm^{-1} results, as compared with a measured value of $E \simeq 30$ V cm^{-1} from figure 3(*a*) which is in reasonable agreement.

Therefore, from the foregoing results, it is inferred that above a certain threshold value a decay instability at the ion-sound frequency, induced by a large-amplitude Bernstein wave in the plasma, is seen in these experiments. Further, for input powers much above threshold, a whole spectrum of instabilities in the range ω_s up to the ion plasma frequency ω_i is observed. Consequently, this suggests the possibility of heating ions by this technique in which energy is transferred from the electron modes into the ion modes via this coupling mechanism and is dissipated by ion collisions. Experiments are continuing on this aspect of the research.

UKAEA Research Group
Culham Laboratory
Berks, England

B E Keen
W H W Fletcher
23rd April 1971

BERNSTEIN, I. B., 1958, *Phys. Rev.*, **109**, 10.
BUCHSBAUM, S. J., and BROWN, S. C., 1957, *Phys. Rev.*, **106**, 196.
CRAWFORD, F. W., 1961, *Phys. Rev. Lett.*, **6**, 663.
DUBOIS, D. F., and GOLDMAN, M. V., 1965, *Phys. Rev., Lett.*, **14**, 544.
HIROE, S., and IKEGAMI, H., 1967, *Phys. Rev. Lett.*, **19**, 1414.
JACKSON, E. A., 1967, *Phys. Rev.*, **153**, 230.
LISITANO, G., 1966, *Proc. 7th Int. Conf. on Phenomena in Ionized Gases, Belgrade*, 1965, Vol 1. (Belgrade: Gradjevinska Kujiza Publishing House), p. 464.
POMEAU, Y., 1967, *Phys. Fluids*, **10**, 2695.
PORKOLAB, P. M., and CHANG, R. P. H., 1969, *Phys. Rev. Lett.*, **22**, 826.
SILIN, V. P., 1965, *Zh. eksp. teor fiz.*, **48**, 1679.
STERN, R. A., 1969, *Phys. Rev. Lett.*, **22**, 767.
STERN, R. A., and TZOAR, 1966, *Phys. Rev. Lett.*, **17**, 903.
TSYTOVICH, V. N., 1970, *Non-linear effects in a Plasma* (New York: Plenum Press).
TZOAR, N., 1969, *Phys. Rev.*, **178**, 356.
WONG, A. Y., BAKER, D. R., and BOOTH, N., 1970, *Phys. Rev. Lett.*, **24**, 804.

N-photon factorial moments for superposition of coherent and chaotic fields

Abstract. The first and the second N-photon factorial moments for the superposition of coherent and chaotic fields and the third N-photon factorial moment for the chaotic field are given for arbitrary spectrum and counting time intervals.

There has been recent interest in multi-photon counting statistics (Teich and Diament 1969, Jaiswal and Agarwal 1969, Barashev 1970a,b, Mišta and Peřina 1970). It was shown that in a counting experiment with an N-photon detector and quasi-monochromatic stationary field one can measure the N-photon counting distribution $p_N(n, T)$ and its factorial moments which are equal to

$$\sum_{n=0}^{\infty} p_N(n, T) \frac{n!}{(n-k)!} = \langle W_N^k \rangle = \beta_N^k \int_{0\ldots}^{T} \int \langle I^N(t_1) I^N(t_2) \ldots I^N(t_k) \rangle \, \mathrm{d}t_1 \ldots \mathrm{d}t_k \qquad (1)$$

where $I(t)$ is an instantaneous intensity of incident field, β_N is the photoefficiency of the N-photon detector and T is the counting time interval.

If the incident field is the linearly polarized superposition of coherent and chaotic fields then it is possible to calculate moments (1) by means of the slightly modified graphical method proposed in Peřina and Mišta (1968). For $k = 1$ and $k = 2$ we obtain

$$\langle W_N \rangle = \beta_N T \sum_{l=0}^{N} \binom{N}{l}^2 l! \, I_{\mathrm{c}}^{N-l} I_{\mathrm{Ch}}^{l} \qquad (2)$$

and

$$\langle W_N^2 \rangle = \beta_N^2 (N!)^4 \sum_{l_1=0}^{N} \sum_{l_2=0}^{N} \sum_{l_3=0}^{\min\{(N-l_1),(N-l_2)\}} \sum_{l_4=0} I_{\mathrm{Ch}}^{l_1+l_2+l_3+l_4} I_{\mathrm{c}}^{2N-l_1-l_2-l_3-l_4}$$

$$\left\{ \prod_{i=1}^{4} l_i! \, (N-l_1-l_3)! \, (N-l_1-l_4)! \, (N-l_2-l_3)! \, (N-l_2-l_4)! \right\}^{-1}$$

$$\int_0^{\mathrm{T}} \int \gamma_{\mathrm{Ch}}^{l_3}(t_1-t_2) \gamma_{\mathrm{Ch}}^{l_4}(t_2-t_1) \gamma_{\mathrm{c}}^{l_3}(t_2-t_1) \gamma_{\mathrm{c}}^{l_4}(t_1-t_2) \, \mathrm{d}t_1 \, \mathrm{d}t_2 \qquad (3)$$